JSLHR

Research Article

Postnatal Development of the Mouse Larynx: Negative Allometry, Age-Dependent Shape Changes, Morphological Integration, and a Size-Dependent Spectral Feature

Tobias Riede,[a,b] Megan Coyne,[b] Blake Tafoya,[b] and Karen L. Baab[c]

Purpose: The larynx plays a role in swallowing, respiration, and voice production. All three functions change during ontogeny. We investigated ontogenetic shape changes using a mouse model to inform our understanding of how laryngeal form and function are integrated. We understand the characterization of developmental changes to larynx anatomy as a critical step toward using rodent models to study human vocal communication disorders.
Method: Contrast-enhanced micro-computed tomography image stacks were used to generate three-dimensional reconstructions of the CD-1 mouse (*Mus musculus*) laryngeal cartilaginous framework. Then, we quantified size and shape in four age groups: pups, weanlings, young, and old adults using a combination of landmark and linear morphometrics. We analyzed postnatal patterns of growth and shape in the laryngeal skeleton, as well as morphological integration among four laryngeal cartilages using geometric morphometric methods. Acoustic analysis of vocal patterns was employed to investigate morphological and functional integration.
Results: Four cartilages scaled with negative allometry on body mass. Additionally, thyroid, arytenoid, and epiglottic cartilages, but not the cricoid cartilage, showed shape change associated with developmental age. A test for modularity between the four cartilages suggests greater independence of thyroid cartilage shape, hinting at the importance of embryological origin during postnatal development. Finally, mean fundamental frequency, but not fundamental frequency range, varied predictably with size.
Conclusion: In a mouse model, the four main laryngeal cartilages do not develop uniformly throughout the first 12 months of life. High-dimensional shape analysis effectively quantified variation in shape across development and in relation to size, as well as clarifying patterns of covariation in shape among cartilages and possibly the ventral pouch.
Supplemental Material: https://doi.org/10.23641/asha.12735917

Shape differences between newborn and adult humans in laryngeal structure are well-established (e.g., Dalal et al., 2009; Eckenhoff, 1951; Holzki et al., 2018; Litman et al., 2003; Tobias, 2015), but the timing on which those changes occur, how changes are manifested in different laryngeal cartilages, and the impact of genetic and environmental effects are unclear. The goal of this study was to investigate how larynx shape, size, and function are related throughout ontogeny. Focusing on the cartilaginous framework, we quantified postnatal size and shape changes of the laboratory mouse (*Mus musculus*) larynx through a cross-sectional study design.

Developmental biology of the larynx in the mouse and rat is highly relevant to both healthy and disordered human activity, as the rodent larynx is a model for studying laryngeal neuromuscular (e.g., Haney et al., 2020; Montalbano et al., 2019) and connective tissue (e.g., Lungova et al., 2015; Peterson et al., 2013; Welham et al., 2015) maturation and injury. Additional applications of rodent models relevant for human health include chronic electronic

[a]Department of Physiology, College of Graduate Studies, Midwestern University, Glendale, AZ
[b]College of Veterinary Medicine, Midwestern University, Glendale, AZ
[c]Department of Anatomy, College of Graduate Studies, Midwestern University, Glendale, AZ
Correspondence to Tobias Riede: triede@midwestern.edu

Editor-in-Chief: Bharath Chandrasekaran
Editor: Michelle Ciucci
Received February 18, 2020
Revision received April 1, 2020
Accepted May 26, 2020
https://doi.org/10.1044/2020_JSLHR-20-00070

Disclosure: *The authors have declared that no competing interests existed at the time of publication.*

This work is licensed under a Creative Commons Attribution-NonCommercial-NoDerivatives 4.0 International License.
Downloaded from: https://pubs.asha.org Midwestern University, Illinois on 05/26/2021, Terms of Use: https://pubs.asha.org/pubs/rights_and_permissions

stimulation of the rat thyroarytenoid muscle for voice disorder therapy (McMullen et al., 2011) and characterizing dysphagia in a rat model for Parkinson disease (Russell et al., 2013). Laryngeal and tracheal pathologies also affect children (e.g., laryngomalacia, vocal fold paralysis; Sittel, 2014), and there is potential for the extension of rodent models to laryngeal developmental research. This study appreciates human laryngeal behavior in the comparative context of mammalian behavior. Our research efforts specifically contribute to recent efforts to characterize rodent laryngeal anatomy for biomedical research (e.g., Lungova et al., 2015; Thomas et al., 2009; Watts et al., 2011) by characterizing development of the laryngeal cartilaginous skeleton in several rodent species employing novel methodology to address questions of growth and function.

In mice, like in other mammals, the larynx is part of the upper respiratory system and involved in swallowing, respiration, and voice production. All three functions are associated with developmental milestones (see Figure 1A) such as feeding transitions from suckling to solid food uptake (e.g., Turman, 2007). In addition, the brain stem circuitry controlling breathing behavior shows important maturation during the first 14 days of life (Dutschmann et al., 2009) and pup vocal behavior during the early postnatal phase (Branchi et al., 2001) is replaced by adult vocal patterns starting after weaning (Brudzynski, 2018; Campbell et al., 2014; Dent et al., 2018).

Movements of the larynx cartilaginous framework control the size of the glottal valve and vocal fold tension. In rodents, intrinsic laryngeal muscle activity is precisely coordinated with the breathing cycle (Riede, 2011), swallowing (Sang & Goyal, 2001), and vocalizations (Riede, 2013, 2018). We therefore hypothesized that there would be noticeable shape changes of the laryngeal framework associated with functional changes of the upper respiratory tract through ontogeny.

While our understanding of laryngeal cartilage function has much advanced (Titze, 2000), our understanding of genetic effects on postnatal development of size and shape is limited. Investigation of ontogenetic development of the larynx is an important step toward deciphering the etiology of laryngeal pathologies with age-specific onsets. Neither the postnatal development of individual laryngeal cartilages nor their integrated development is well understood. Furthermore, genetic and/or environmental factors determining morphological shape variation are poorly understood; however, both embryological origin and functional constraints are hypothesized to influence correlated development of morphological structures (Olson & Miller, 1958). In general, the developmental interaction among cells, tissues, and their environment determines ontogenetic trajectories (e.g., Hallgrímsson et al., 2007). Phenotypic interdependence of two or more structures (here cartilages) could reflect common function or development (Olson & Miller, 1958). Recent work illustrated that laryngeal cartilages and muscles are of mixed embryonic origins (Heude et al., 2018; Tabler et al., 2017; see Figure 1B). The current study will also address whether postnatal developmental interactions between laryngeal cartilages is more closely linked to embryonic origin or function.

The rodent larynx is one of the smallest vocal organs. Previous investigations suggested that overall postnatal development remained limited to a simple increase in larynx size (Alli et al., 2013; Thomas et al., 2009), but those studies failed to capture nuances in shape variation. Modern imaging approaches allow the generation of three-dimensional (3D) reconstructions of the rodent larynx (Riede et al., 2017), and geometric morphometric analysis provides the means for a thorough ontogenetic shape analysis (Adams, 2016; Klingenberg, 2016), including the larynx (Borgard et al., 2019). This study has combined a quantitative analysis of postnatal growth patterns in four laryngeal cartilages in CD-1 mice using 3D geometric morphometrics in order to test two hypotheses. Firstly, we investigated whether laryngeal growth was associated with characteristic changes in shape of individual cartilages. Secondly, we tested whether cartilage shapes vary (semi-) independently of other cartilages or whether shape change across cartilages is strongly integrated. We also investigated the relationship of acoustic properties to changes in cartilage size and shape.

Method

Animals

A total of 24 animals (CD-1 mouse, *Mus musculus*) were investigated, which included 2-day-old (N = 3 males, 3 females; hereafter "pups"), 21-day-old (N = 3 males, 3 females; hereafter "weanlings"), 90-day-old (N = 3 males, 3 females; hereafter "young adults"), and 365-day-old (N = 3 males, 3 females; hereafter "old adults") animals. The age phase between 10 and 15 months correlates to humans from 38–47 years old (Flurkey et al. 2007). The known-age individuals were bred from colonies maintained at Midwestern University. The old adult animals were retired breeders. The samples were genetically heterogeneous by selecting only one male and one female from a certain litter. All procedures were in accordance with the National Institutes of Health guidelines for experiments involving vertebrate animals and were approved by the Institutional Animal Care and Use Committee at Midwestern University, Glendale, Arizona.

Tissue Preparation, Imaging, and 3D Reconstruction

Animals were euthanized with Ketamine/Xylacine and exsanguinated by transcardial perfusion with 0.9% saline, chased with 10% buffered formalin phosphate (SF100-4; Fisher Scientific). Larynges were then dissected and kept in 10% buffered formalin phosphate for 12 hr and then in 99% ethanol for another 24 hr. Each specimen was then stained in 1% phosphotungstic acid (Sigma-Aldrich, 79690) in 70% ethanol. After 5 days, the staining solution was renewed and the tissue was stained for another 5 days. Stained specimens were placed in a custom-made acrylic tube, stabilized with polystyrene craft foam and scanned in

Downloaded from: https://pubs.asha.org Midwestern University, Illinois on 05/26/2021, Terms of Use: https://pubs.asha.org/pubs/rights_and_permissions

Figure 1. (**A**) The postnatal development of the mouse features several important steps that directly or indirectly involve the larynx. For example, pups eventually transition from suckling to solid food or young mice eventually develop a complex adult vocal behavior that includes songs and various call types (Holy & Guo, 2005). (**B**) The larynx cartilage framework originates from neural crest and mesoderm (Tabler et al., 2017). Line art on the left indicates the in vivo positioning of four laryngeal cartilages. The "blown-up" illustration on the right indicates the two tissue sources that contribute to the larynx development. (**C**) Position of fixed curve (open circles) landmarks used in this study. See Table 1 for explanation of curve landmarks and surface (small black dots) landmarks.

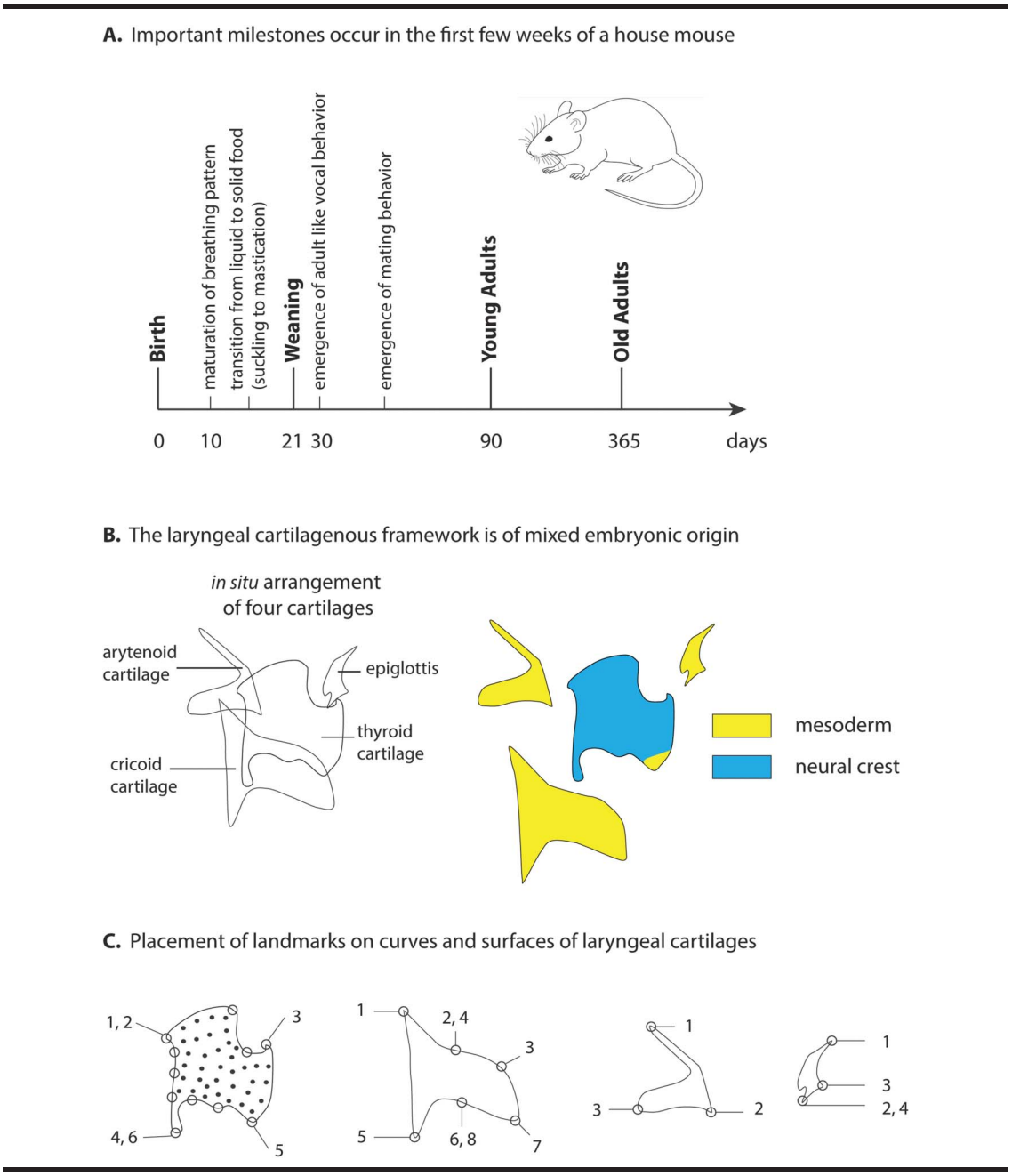

air with 59-kV source voltage and 167-μA intensity using a Skyscan 1172 (Bruker-microCT). Projection images were recorded with an angular increment of 0.4° over a 180° rotation. Voxel size in the reconstructed volumes ranged between 4.8 and 5.1 μm per pixel. Reconstructed image stacks were then imported into AVIZO software (Version Lite 9.0.1). Laryngeal cartilages and the border between the airway and soft tissues of the larynx in the computed tomography scans were segmented manually to provide an outline of the cartilaginous framework. Derived 3D surfaces (stereolithography format) of all specimens are available on Morphobank (O'Leary & Kaufman, 2012), Project 3635.

Downloaded from: https://pubs.asha.org Midwestern University, Illinois on 05/26/2021, Terms of Use: https://pubs.asha.org/pubs/rights_and_permissions

Table 1. Definition of fixed curve landmarks on laryngeal cartilages.

	Thyroid cartilage
1	Posterior most point on rostral margin of left cranial process
2	Midline point on cranial margin
3	Posterior most point on cranial margin of right cranial process
4	Posterior most point on caudal margin of right caudal process
5	Midline point on caudal margin
6	Posterior most point on caudal margin of left caudal process
	Cricoid cartilage
1	Posterior most point on cranial margin
2	Most left point on cranial margin
3	Anterior most point on cranial margin
4	Most right point on cranial margin
5	Posterior most point on caudal margin
6	Most left point on caudal margin
7	Anterior most point on caudal margin
8	Most right point on caudal margin
	Arytenoid cartilage
1	Most distal point on cranial process
2	Most distal point on vocal process
3	Most distal point on muscular process
	Epiglottis
1	Most cranial point along midsagittal line
2	Most left point on lateral margin
3	Most caudal point along midsagittal line
4	Most right point on lateral margin

Note. Gliding landmarks were added between those landmarks.

Landmark Selection

We used fixed and sliding curve landmarks as well as surface landmarks to define the shape of four laryngeal cartilages (see Table 1 and Figure 1C). One hundred surface landmarks were acquired from the thyroid and cricoid cartilages, and 50 from the arytenoid cartilage and the epiglottis to achieve comprehensive coverage. We established the optimal number of landmarks for each cartilage previously (Borgard et al., 2019).

Landmark placement was performed in R 3.4.4 (R Core Team, 2015) using the *geomorph* package (Adams et al., 2017). The procedure of placing landmarks is interactive. First, a point is selected on the surface rendering of the cartilage using the cursor, and then the user confirms to keep or discard the selected point before the next point can be selected.

The coordinate data of all selected points were then superimposed using generalized Procrustes analysis for each set of landmarks analyzed (Gower, 1975; Rohlf & Slice, 1990). For each cartilage, the generalized Procrustes analysis procedure first translates all landmark configurations to the origin (0, 0, 0), then scales all landmark configurations to unit centroid size (i.e., it removes raw scale differences), and finally rigidly rotates landmark configurations to minimize squared distances across corresponding landmarks (Baab et al., 2012). This produces a set of transformed coordinates that reflect shape differences among cartilages independent of scaling.

Acoustic Recording and Analysis

In order to test whether morphological shape changes of the vocal organ are associated with vocal behavior, we made sound recordings of vocal behavior. Three age groups were audio-recorded before they were sacrificed. Pups were isolated from their litter for 5 min and placed into a large petri dish that was heated to a temperature of 28°C. The microphone (Type CM16/CMPA-5V; 15–180 kHz, with a flat frequency response [± 6 dB] between 25 and 140 kHz; Avisoft Bioacoustics) was placed 5 cm above the dish.

Unfortunately, recording attempts of weanlings were unsuccessful. Young and old adult mice were recorded while being socially housed and acoustically monitored for 48 hr. Spontaneous vocalizations were recorded. Vocalizations in adult mice were also triggered by providing soiled bedding from the opposite sex. The microphone was placed 5 cm above the cage (20 × 31 × 13 cm). The microphone distance relative to the animal changed because the animals moved around inside the cage. The microphone signal was digitized by an ultrasound recording interface (UltraSoundGate 416H, Avisoft Bioacoustics) and using Avisoft recording software (Avisoft Recorder USGH) with a 300-kHz sampling rate. Sound recordings were processed (1,024-point Fast Fourier Transform, 75% frame size, Hann window, frequency resolution 100 Hz, temporal resolution 0.625 ms; 2–120 kHz bandpass filtered). The analysis focused on fundamental frequency (F0), which was quantified every 5 ms using the *pitch tracking* module of the Praat software (v. 5.2.12). Pitch tracking results were visually confirmed by overlaying the tracking contour to the spectrogram. Mismatches, for example, caused by acoustic distortions to the recording caused by sound reflections or animal movement noises, were discarded. Approximately 15,000 tracking points for each age group (which corresponds to 75 s of calls) were collected. F0 data were represented as histograms (30–90 kHz, 500-Hz bin resolution). *Mean F0* was calculated by averaging all 500-Hz frequency bins in the histogram. This weighs different frequency bins according to the rate of their occurrence. *F0 range* represents the F0 range containing 50% of tracking points equally distributed around the *mean F0*.

Statistical Analysis

Size

Body size was estimated through body mass and left femur length. We used centroid size as a univariate measure of overall size for each cartilage. Centroid size is the most common measure of size in geometric morphometrics (Rohlf & Slice, 1990). Centroid size is computed as the square root of the sum of squared distances of each landmark from the centroid, which is calculated by averaging the *x, y,* and *z* coordinates of all landmarks (Zelditch et al., 2004). As an analogy, one could think of it as the average distance of landmarks to the centroid or the center of mass of each cartilage.

Four additional linear measures were taken from each specimen: (a) diameter of the airway measured at the caudal end of the cricoid cartilage, (b) membranous vocal

Downloaded from: https://pubs.asha.org Midwestern University, Illinois on 05/26/2021, Terms of Use: https://pubs.asha.org/pubs/rights_and_permissions

fold length measured between the vocal process of the arytenoid cartilage and the ipsilateral protuberance on the medial surface of the thyroid cartilage, (c) largest latero-lateral distance of the ventral pouch, and (d) largest rostro-caudal dimension of the ventral pouch entrance (also known as "A1" distance; Riede et al., 2017). All four measures were taken using the linear measure tool in AVIZO. Airway diameter and vocal fold length are standard size metrics used in the literature on larynx morphology and provide a point of comparison with previous studies. Ventral pouch geometry has been suggested to be a critical determinant of F0 of ultrasonic vocalizations (Riede et al., 2017). Two-way analysis of variance (sex and age) was used to analyze sexual dimorphism in size.

The investigation of ontogenetic scaling studies the relationship between stages of development of an organism and the size of its parts; in other words, as the mouse grows, do all cartilages of the larynx grow proportionately? For example, some cartilages may grow very little while others grow steadily over the same time period while still others show a punctuated pattern of growth. Ontogenetic scaling relationships of laryngeal cartilage size were analyzed using ordinary least squares regression of $\log_{10}$-transformed centroid size on $\log_{10}$ (body mass [BM]). For cartilages to be considered geometrically similar and an isometric scaling pattern to be inferred, a linear trait (femur length, vocal fold length, airway diameter, centroid size) should scale to $BM^{0.33}$ (i.e., the slope of the linear measure scales to $BM^{0.33}$).

Shape

If individual laryngeal cartilages grow in size at different rates, this will cause age-specific shapes of the larynx, potentially with biomechanical consequences. The growth rates of individual cartilages can be isometric or allometric (i.e., the laryngeal proportions can remain constant throughout life or they can change, respectively). We employed a series of principal components analyses (PCAs) to summarize the main patterns of shape variation in the four age groups. PCA is a data reduction technique that summarizes the major patterns of variation in highly multivariate data sets. The PCA was performed on the superimposed landmark data, and the first two axes (Principal Components 1 and 2 [PC 1 and PC 2]) were used to illustrate relationships (similarity) among age groups. Shape variation along PC axes were generated by first identifying the specimen closest to the mean shape and then warping it to the mean shape using the "warpRefMesh" function in *geomorph*. The loadings for each PC axis were added and subtracted from the mean shape to produce the shapes at the positive and negative ends of each axis, respectively, using the "PlotTangentSpace" function in *geomorph*.

A multivariate analysis of variance was performed on the PC 1 and PC 2 scores for each cartilage to determine whether age groups and sexes were statistically distinguishable on the basis of cartilage shape.

Integration and Modularity

Morphological integration refers to the interdependence of structures that reflect common genetic, developmental, or functional factors. Morphological integration can be viewed as a network with connections among traits varying in their intensity. Modularity refers to the case where this network is organized into clusters of strongly integrated traits (modules), which are less strongly integrated with other modules (Wagner, 1996). A network with more-or-less equal strength of integration among all traits is more integrated and less modular. The advantage of a modular organization in evolutionary terms is that it facilitates semi-autonomous evolution of linked traits. We tested the hypothesis that each of the four cartilages represents a distinct module with stronger covariances among, for example, all cricoid landmarks than between cricoid and thyroid landmarks. We used the covariance ratio (CR; Adams, 2016), which measures the strength of between-module covariation relative to within-module covariation. The CR was estimated using the "modularity.test" function in the package *geomorph*. The CR ranges between 0 and positive values. Values near 1 indicate that the level of covariation between cartilages is, on average, the same as the covariation within a cartilage and thus the two cartilages are not modular. Values closer to 0 (< 1) indicate that the degree of covariation between modules is less than that found within modules and is interpreted as evidence of a modular organization. Statistical significance of the pairwise CR values calculated for all cartilages is tested against a null hypothesis of randomly assigning landmarks to each module. A resampling procedure that randomly assigns landmarks to each module produces an empirical distribution against which the observed CR can determine statistical significance (Adams, 2016). The expected value for this distribution is 1, as the levels of covariation should be the same within and between modules in this scenario. We then calculated the effect size (z score) for each CR value and compared these values for each pair of cartilages to determine which pairs, if any, are more modular than others using the "compare.CR" function in the package *geomorph* (Adams & Collyer 2019). Additional methodological details can be found in the Supplemental Material S1.

Results

Size

Body mass increased from one age group to the next by 66.3%, 61.9%, and 37.7%, respectively. Femur length increased by 43.6%, 31.2%, and 7.8% (as measured by femur length), respectively (see Figure 2A). The lengths of the left femur scaled with moderate positive allometry ($\beta = 0.39$, $r = .97$, $p < .001$; expected slope [β] representing isometry would be 0.33; see Figure 2B). Airway diameter and vocal fold length scaled with negative allometry on body mass (airway diameter: $\beta = 0.22$, $r = .97$, $p < .001$; vocal fold: $\beta = 0.16$, $r = .79$, $p < .001$; see Figures 2C and 2D). Latero-lateral diameter of the ventral pouch did not scale with body mass or thyroid cartilage centroid size (latero-lateral distance on body mass: $\beta = 0.06$, $r = .37$, $p = .24$; on thyroid

Downloaded from: https://pubs.asha.org Midwestern University, Illinois on 05/26/2021, Terms of Use: https://pubs.asha.org/pubs/rights_and_permissions

Figure 2. Size and shape development of four laryngeal cartilages throughout the first year. Measurements were taken in four age groups (2 days, 21 days, 90 days, and 365 days) from six individuals (three males) in each group. (**A** and **B**) Body mass and femur length increase with age, and both variables are tightly associated. (**C** and **D**) Airway diameter and vocal fold length (VFL) scale allometrically with body mass. (**E**–**H**) The size of each of the four cartilage scales also allometrically with overall body size. (**I**–**L**) Principal components analysis ordinations summarizing major axes of shape variation for the thyroid, cricoid, arytenoid, and epiglottic cartilages. Note the nonlinear developmental trajectories of the arytenoid and epiglottic cartilages and the minimal shape differentiation among developmental stages for the cricoid cartilage. (**M**–**P**) Except for the cricoid cartilage, a substantial portion of the shape variation is explained by the first and second principal components. (**Q**–**T**) Shape changes captured by PC 1 are correlated with size for the thyroid, arytenoid, and epiglottic cartilages, but not for the cricoid cartilage. PC = principal component; LL = largest latero-lateral distance of the ventral pouch; RC = largest rostro-caudal dimension of the ventral pouch entrance.

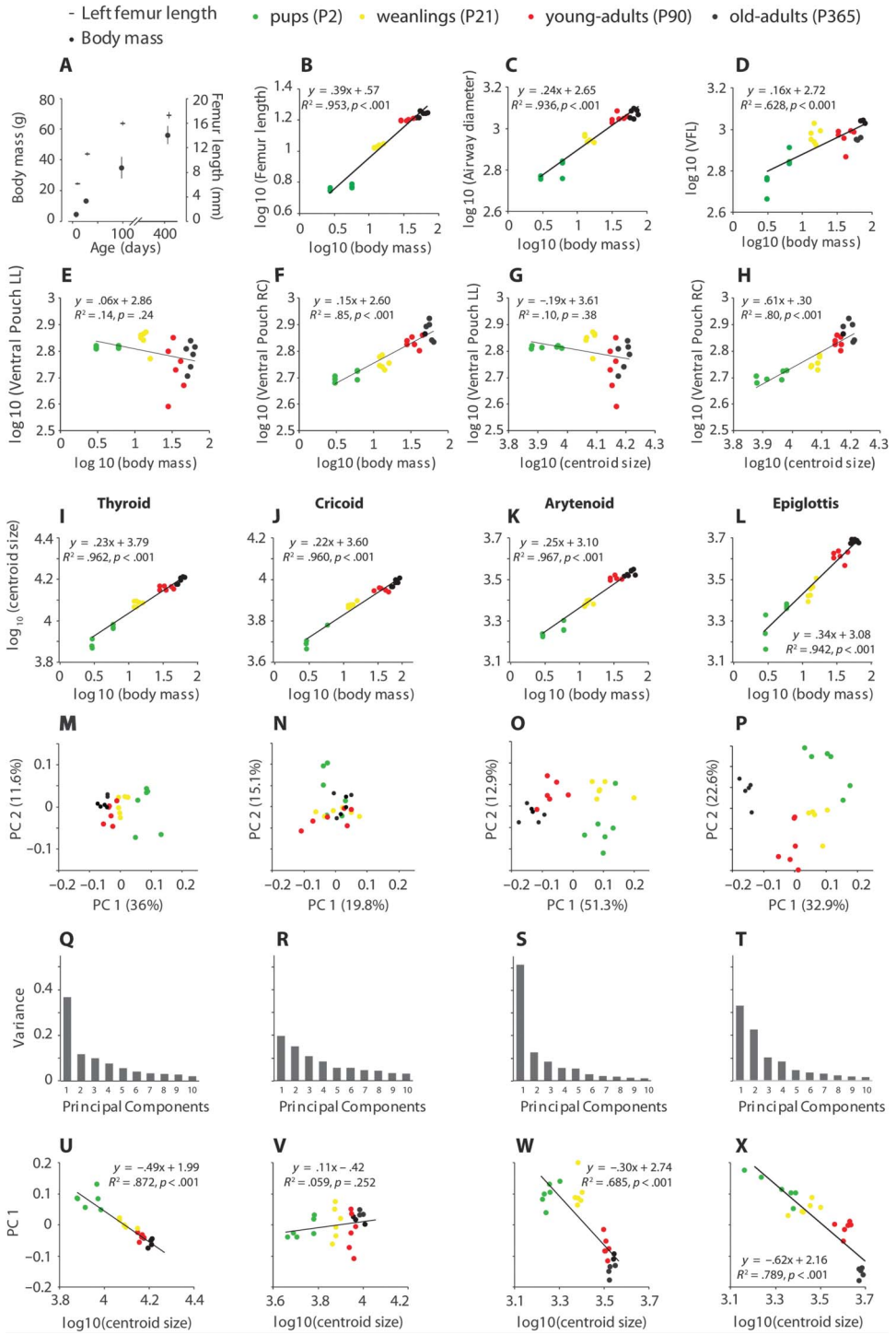

Downloaded from: https://pubs.asha.org Midwestern University, Illinois on 05/26/2021, Terms of Use: https://pubs.asha.org/pubs/rights_and_permissions

cartilage centroid size: $\beta = -0.19$, $r = .32$, $p = .38$; see Figures 2E and 2G). The rostro-caudal length of the ventral pouch scaled with negative allometry on body mass and thyroid cartilage centroid size (rostro-caudal distance on body mass: $\beta = 0.15$, $r = .92$, $p < .001$; on thyroid cartilage centroid size: $\beta = 0.61$, $r = .89$, $p < .001$; see Figures 2F and 2H).

Centroid sizes of the four larynx cartilages also scaled with negative allometry on body mass. The epiglottis had the least marked negative allometric exponent ($\beta = 0.31$, $r = .97$, $p < .001$), while the allometric scaling of thyroid, cricoid, and arytenoid cartilages was more prominent (β values were 0.23, 0.21, and 0.24, respectively; all three Pearson correlations, $r = .98$, $p < .001$; see Figures 2I–2L).

Shape

A large proportion of shape variation is captured by the first two PCs (PCs 1 and 2), typically ≥ 50% (except for cricoid, where they account for 34%; see Figures 2Q–2T). We investigated whether the four cartilages assumed an age-specific shape by exploring the position of each age group in the subspace of the first two PCs (see Figure 2, Panels M–P).

There was a clear developmental progression captured by PC 1 of thyroid cartilage shape (see Figure 2M). Pups clustered on the positive end of PC 1 opposite from the old adult mice (365 days). The old adult thyroid cartilage showed a greater medio-lateral to dorso-ventral width ratio (see Figures 3A and 3B). Furthermore, the ventral and caudal aspect of the laminae (=ventral rim) was more bent (arrows in lateral view of Figure 3A). The first PC for the thyroid cartilage contributed most (and PC 2 contributed very little) to the separation of age groups (see Figure 2Q). The contribution of the first PC is also illustrated by a strong correlation between the scores of individuals on PC 1 and their centroid sizes (Pearson correlation; $r = -.93$; $p < .001$; see Figure 2U).

Scores on the first and second PCs of cricoid cartilage shape did not differ statistically among four age groups (see Figure 2N) and were not correlated with centroid size (see Figure 2V). Contribution of the first few PCs is shown in Figure 2R.

The four age groups exhibited separation of their arytenoid cartilage shape along the first PC (see Figure 2O), and shape change during development was nonlinear (reflected in the curving trajectory traced from pups to old adults). Pups and weanlings clustered on the positive end of PC 1 opposite from the young and old adult mice. The first PC for the arytenoid cartilage contributed strongly to the separation of age groups (see Figure 2S). Likewise, scores on PC 1 for the arytenoid cartilages were strongly correlated with centroid size (see Figure 2W). Although the second PC did not contribute strongly to separation of age groups, it separates the pups and old adults from weanlings and young adults (see Figure 2O). Two shape features are captured by the first axis of variation. The angle between the apex (dorsal process) and main body (vocal and muscular process) is almost 90° in older mice but at an obtuse angle in younger animals (medial view in Figure 3E). The cartilage also appears to flatten toward body's midline in older animals (arrows in top view of Figure 3E).

With regard to epiglottis shape, pups clustered on the positive end of PC 1 opposite from the old adult mice, while weanlings and young adult mice cluster between them, near the origin (see Figure 2P). Like the arytenoid, epiglottis development is nonlinear. Not surprisingly, variation along PC 1 for the epiglottis was also related to size differences (see Figure 2X). On the second PC axis, pups and old adult mice cluster on the positive end, opposite from the weanlings and young adults (see Figure 2P). The first two components of epiglottis shape contribute to the separation of the age groups (see Figure 2T). The two caudal processes became more prominent in the adult cartilage (see Figures 3G and 3H).

Male and female mice were not statistically distinguishable in the shape of the four cartilages (thyroid cartilage: $F(4, 24) = 1.28$, $p = .294$; cricoid cartilage: $F(4, 24) = 0.55$, $p = .765$; arytenoid cartilage: $F(4, 24) = 1.47$, $p = .221$; epiglottis: $F(4, 24) = 0.44$, $p = .849$). Data were therefore grouped together when we investigated whether any particular laryngeal cartilage represented a more sensitive indicator of age-specific differences. The results of the multivariate analysis of variance indicated that the four age groups were statistically distinguishable in the shape of the thyroid cartilage, $F(4, 24) = 59.9$, $p < .001$, Wilk's $\Lambda = 14.8$, partial $\eta^2 = .7$; cricoid cartilage, $F(4, 24) = 2.4$, $p = .043$, Wilk's $\Lambda = 0.52$, partial $\eta^2 = .279$; arytenoid cartilage, $F(4, 24) = 14.4$, $p < .001$, Wilk's $\Lambda = 0.093$, partial $\eta^2 = .695$; and epiglottis, $F(4, 24) = 33.4$, $p < .001$, Wilk's $\Lambda = 0.025$, partial $\eta^2 = .841$. However, the very low partial η^2 value for the cricoid suggests that cricoid shape does not discriminate among age groups as well as the other cartilages. This is consistent with the minimal separation of age groups apparent in the subspace of PCs 1 and 2 described above.

The magnitude of shape change that occurred between adjacent age categories differed among the four cartilages. For example, there was a larger gap between weanlings and young adults with regard to the arytenoid and epiglottic cartilages (see Figures 2W and 2X) than thyroid and cricoid cartilages (see Figures 2U and 2V). We estimated Euclidean distances between adjacent age-group centroids in the PC 1–PC 2 subspace (larger distances indicate a higher magnitude of shape differences). For the thyroid cartilage, distances decreased with increasing age (see Figure 4A), suggesting that most shape change is concentrated early in development. The cricoid cartilage experienced overall low magnitudes of shape change throughout the first year, suggesting that cricoid shape does not change substantially throughout development. The arytenoid cartilage showed the largest change after weaning, which may reflect the many behavioral changes that occur after weaning related to breathing, feeding, vocalization, and locomotion/movement patterns. The epiglottis shows relatively large shape changes throughout the first year. On average, shape changes for thyroid and cricoid cartilages were smaller than for arytenoid cartilage and epiglottis (see Figure 4B).

Integration and Modularity

We calculated covariances for landmarks from all four cartilages to test for the presence of a modular signal

Downloaded from: https://pubs.asha.org Midwestern University, Illinois on 05/26/2021, Terms of Use: https://pubs.asha.org/pubs/rights_and_permissions

Figure 3. Warped cartilage images showing shape changes. Images represent shape changes associated with the minimum and maximum extents of PC 1 and PC 2 for the thyroid (A, B), cricoid (C, D), arytenoid (E, F) cartilage, and epiglottis (G, H). PC = principal component.

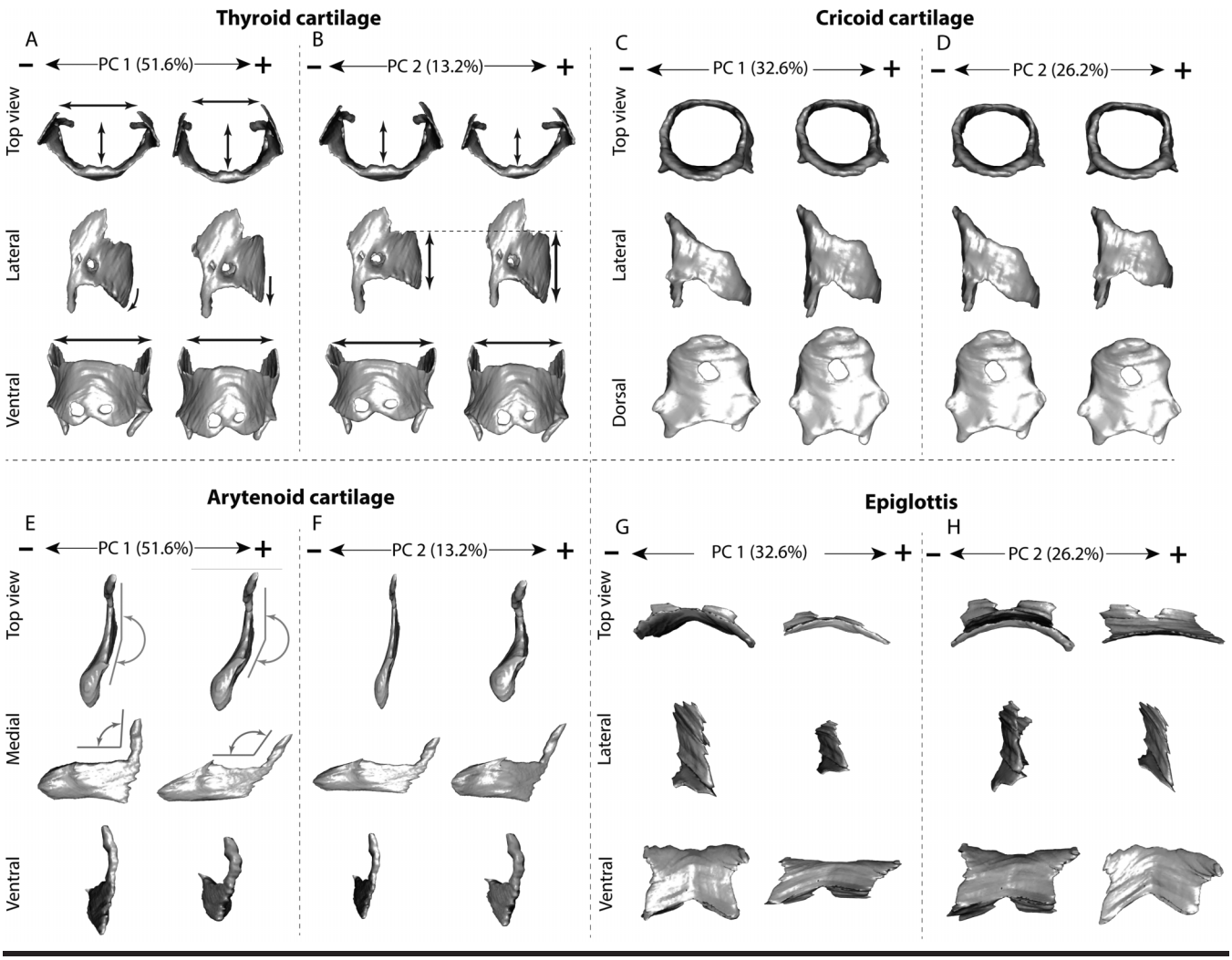

Figure 4. (**A**) Euclidean distance between cluster centroids of PC scores (PC 1 and PC 2) of four age groups. A large distance for example between weanlings (P21) and young adults (P90) for the arytenoid cartilage, indicates a large change in shape. (**B**) Average distance between adjacent developmental stages for each of the four cartilages (mean ± standard deviation). T = thyroid cartilage; C = cricoid cartilage; A = arytenoid cartilage; E = epiglottis; PC = principal component.

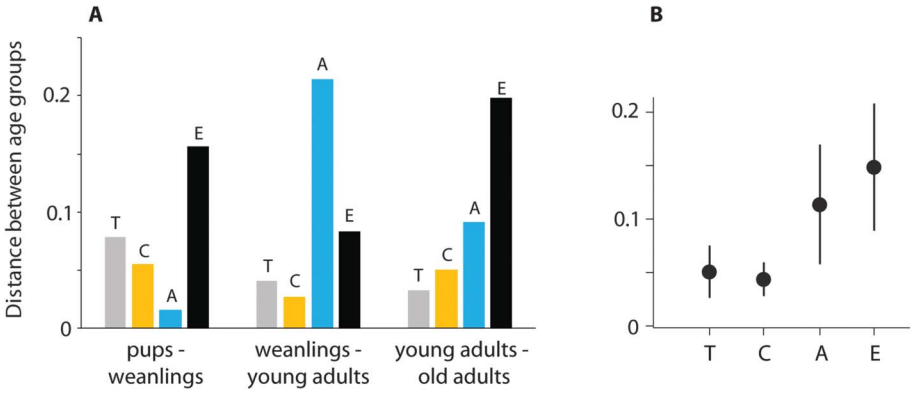

Downloaded from: https://pubs.asha.org Midwestern University, Illinois on 05/26/2021, Terms of Use: https://pubs.asha.org/pubs/rights_and_permissions

in the data. Specifically, we assessed whether landmarks from each cartilage (our a priori modules) covaried more strongly with each other than with landmarks from another cartilage through the CR. All CR values were significantly lower than 1 (see Table 2), confirming greater modularity (independence) among the four cartilages than expected by chance.

Next, we calculated the effect size (z score; Z_{CR}) for each CR and tested for statistically significant differences among the pairs of cartilages to determine which pairs, if any, had a stronger modularity signal than others. Effect sizes are useful for evaluating not just statistical significance, but magnitude or size of the effect. In our case, the more negative the Z_{CR} value, the stronger the modularity signal. The thyroid and cricoid cartilages had the largest effect sizes, and thus the strongest signal of modularity, followed by the thyroid and arytenoid cartilages (see Table 3). Indeed, the most consistent result is that the pairs of cartilages, which include the thyroid, are generally more modular than other pairs, suggesting that the thyroid had the most independent shape development of the four cartilages.

Acoustic Analysis

Mean F0 (*mean F0*) and F0 range (*F0-range*) for three age groups (see Table 4) provided insufficient statistical power; however, the results are suggestive and provide insight for future hypothesis testing. *Mean F0* decreases with size (see Figure 5), which follows the expected size-dependent change in F0. While the relationship between *mean F0* and all size measures are suggestive of a negative association, the correlations between *F0-range* and size parameters do not follow the same trend (see Figure 5D and Table 4). Relating both F0 measures to the second PC seems to support a relationship between cartilage shape and frequency (see Figure 5D and Table 5). While *mean F0* is more strongly correlated with scores on the first axis, *F0-range* relates more strongly to position along the second shape axis (see Table 5). The first result is not surprising as both PC 1 scores and *mean F0* are correlated with size. The latter result suggests a relationship between *F0-range* and shape, perhaps reflecting functional morphological adaptations.

Discussion

We captured ontogenetic size and shape changes of the mouse larynx by combining contrast-enhanced micro-computed-tomographic imaging, 3D reconstruction, and geometric morphometric analysis. There are six main results of this cross sectional analysis: (a) All four cartilages as well as airway diameter, vocal fold length, and one ventral pouch dimension scaled with negative allometry on body size. (b) All cartilages with the exception of the cricoid also demonstrated age-dependent shape changes. (c) The rate at which shape changed varied among the four cartilages. (d) All cartilages were confirmed as distinct modules but with varying degrees of independence from one another. The variation may reflect the mixed embryological origin of the vocal organ since the thyroid cartilage was most autonomous in its development and has a distinct embryological origin from neural crest cells (Tabler et al., 2017). (e) Mean F0 was associated with larynx size, while F0 range may relate somehow to cartilage and ventral pouch shape. (f) Ventral pouch geometry suggests an unexpected shape maturation. While its rostro-caudal dimension scaled with overall size, its latero-lateral dimension did not.

Negative Allometric Growth of Larynx and Laryngeal Airway

The laryngeal cartilages and airway are relatively larger in pups than in adult mice. This finding complements our understanding of negative allometric scaling of the tracheal and bronchial airway diameter across species (Holzki et al., 2018; Mortola & Fisher, 1980; Tenney & Bartlett, 1967; Valerius, 1996). Mammals rely on their lungs for gas exchange, but air needs to be transported through the conducting airways, which do not participate in gas exchange, before air reaches the respiratory airways. Moving air into the lungs is associated with a cost for the work to overcome airway resistance. Airway resistance is dictated by airway diameter, including the size of the laryngeal lumen. Flow resistance inside a tube-like structure is inversely proportional to the fourth power of its radius (Poiseuille's Law; i.e., the smaller the airway diameter the greater the resistance). Increased diameter of the conducting airway would decrease airway resistance but also increase the anatomical dead space. The tradeoff between the work load associated with lung ventilation and the size of the conducting airways appears to have favored relatively wider airways and a reduced airway resistance in smaller animals.

We did not observe sexual dimorphism in cartilage shape. This contrasts with previously reported differences

Table 2. Covariance ratio coefficients (CR) and effect size (Z_{CR}) obtained from a permutation test of alternative partitions of the pairs of two laryngeal cartilages under the hypothesis of no modularity

Cartilage	Thyroid	Cricoid	Arytenoid
Cricoid	Z_{CR} = –27.5, CR = 0.717; p = .001		
Arytenoid	Z_{CR} = –24.2, CR = 0.804; p = .001	Z_{CR} = –20.9, CR = 0.650; p = .001	
Epiglottis	Z_{CR} = –21.5, CR = 0.851; p = .001	Z_{CR} = –15.0, CR = 0.854; p = .001	Z_{CR} = –10.7, CR = 0.858; p = .001

Downloaded from: https://pubs.asha.org Midwestern University, Illinois on 05/26/2021, Terms of Use: https://pubs.asha.org/pubs/rights_and_permissions

Table 3. The covariance ratio effect sizes (Z_{CR}) were further compared for evaluation of modularity (Adams & Collyer, 2019).

Variable	TC (Z_{CR} = −27.5)	TA (Z_{CR} = −24.2)	TE (Z_{CR} = −21.5)	CA (Z_{CR} = −20.9)	CE (Z_{CR} = −15.0)
TA (Z_{CR} = −24.2)	**$\hat{Z}$ = −2.29, p = .022**				
TE (Z_{CR} = −21.5)	**$\hat{Z}$ = −4.21, p < .001**	$\hat{Z}$ = −1.9, p = .054			
CA (Z_{CR} = −20.9)	**$\hat{Z}$ = −4.63, p < .001**	**$\hat{Z}$ = −2.34, p = .019**	$\hat{Z}$ = −0.41, p = .67		
CE (Z_{CR} = −15.0)	**$\hat{Z}$ = −8.81, p < .001**	**$\hat{Z}$ = −6.51, p < .001**	**$\hat{Z}$ = −4.59, p < .001**	**$\hat{Z}$ = −4.17, p < .001**	
AE (Z_{CR} = −10.7)	**$\hat{Z}$ = −11.8, p < .001**	**$\hat{Z}$ = −9.55, p < .001**	**$\hat{Z}$ = −7.62, p < .001**	**$\hat{Z}$ = −7.21, p < .001**	**$\hat{Z}$ = −3.03, p = .002**

Note. The outcome is another effect size value ($\hat{Z}$), which evaluates the strength of the covariance ratio (see Table 2) between two cartilages. For statistically significant comparisons (in bold), the pair with the more negative Z_{CR} has the stronger modularity signal. T = thyroid cartilage; C = cricoid cartilage; A = arytenoid cartilage; E = epiglottis.

between male and female mice in vocal activity as well as in acoustic parameters of their ultrasonic vocalization (Fernández-Vargas, 2018; Zala et al., 2017). This result is unlikely to be an artifact as the high resolution of the landmark/semilandmark sampling should accurately capture even subtle variations in shape. However, it supports the hypothesis that vocal differences in *Mus musculus* are in large part based on differences in neural control (Fröhlich et al., 2017). Future morphometric studies of male and female mouse larynges should include intrinsic musculature (e.g., Hoh, 2005) as well as connective tissue, such as the vocal ligament (e.g., Tateya et al., 2005; Yamashita et al., 2010).

Integrating Ontogenetic Changes in Size, Shape, and Function

Three of four laryngeal cartilages demonstrated a clear ontogenetic trend in shape change as summarized by the first two shape axes. The adult mouse thyroid cartilage shape was characterized by a medio-lateral widening as well as a bending of the ventral rim. The angle between the dorsal process and the main body of the arytenoid became more acute consisting of muscular and vocal processes. Furthermore, the adult arytenoid cartilage appeared flatter than that of pups and weanlings. The adult epiglottis showed a greater angulation toward the laryngeal surface, and the two caudal processes were more prominent in the adult form. Sexual dimorphism of laryngeal cartilage shape was absent.

Table 4. Acoustic parameters (mean fundamental frequency [F0], F0, and F0 range) for three age groups of CD-1 mice.

Age group	Mean F0	F0-range
P2	62.3 kHz	15.0 kHz (55.0–70.0 kHz)
P90	60.5 kHz	13.5 kHz (52.0–65.5 kHz)
P365	54.3 kHz	15.5 kHz (45.5–61.0 kHz)

Note. P2 = age 2 days; P90 = age 90 days; P365 = age 365 days.

The rate of shape change differed among the three cartilages. For example, the arytenoid cartilage showed its most prominent shape change after weaning. The muscular process was originally directed more laterally in pups but is directed more dorsally in adults (see Figure 3E). The arytenoid shape is critical for laryngeal biomechanics (Tayama et al., 2001) since its movement contributes to vocal fold ab- and adduction as well as vocal fold stiffening (Titze, 2000). We hypothesize that the difference in rates reflects specific functional demands in the arytenoid cartilage. In laboratory mice, changes in diet (Turman, 2007), breathing pattern (Dutschmann et al., 2009), and vocal behavior (Brudzynski, 2018) all occur between 10 and 20 days postnatally. Those changes are likely associated with modified demands to glottal abduction and adduction. Our data suggest that those behavioral changes are associated with morphological adaptations. A causal mechanistic relationship remains to be tested experimentally.

Like the arytenoid cartilage, the epiglottic cartilage exhibited marked variation in magnitude of shape change between adjacent age groups, suggesting distinct phases of shape development for these cartilages. This observation explains the nonlinear pattern of shape change indicated by the curvilinear paths of development from pups to old adults seen in Figures 2K and 2L (see Neubauer et al., 2010, for a similar interpretation). It is also worth noting that the "jumps" in shape change do not correspond to comparable "jumps" in cartilage size.

The cricoid cartilage generally shows less variation within and between species, and there was minimal distinction in shape across developmental stages. For example, we previously used the same geometric morphometric approach to demonstrate that the cricoid cartilage showed the least shape differences between five rodent species of all the laryngeal cartilages (Borgard et al., 2019). For the human larynx, we know that there are important age-specific shape characteristics in the pediatric, juvenile, and adult organ (e.g., Eckel et al., 1994, 1999; Kahane, 1982), but

Downloaded from: https://pubs.asha.org Midwestern University, Illinois on 05/26/2021, Terms of Use: https://pubs.asha.org/pubs/rights_and_permissions

Figure 5. Acoustic analysis of pup, young, and old adult vocal behavior. (**A**) Example of a bout of seven isolation calls produced by a 2-day-old pup. Calls are shown as oscillograms (top panel) and spectrograms (bottom panel) and the tracked fundamental frequency (F0; **B**). F0 data points for these calls are displayed as histogram (**B**) showing the occurrence of each frequency between 0 and 90 kHz (500-Hz bins). (**C**) We were able to record calls from each individual in three age groups. F0 data points are displayed as histograms showing the occurrence of each frequency between 0 and 90 kHz (500-Hz bins). (**D**) Mean fundamental frequency (*mean F0*) and fundamental frequency range (*F0-range*) are plotted against mean $\log_{10}$–transformed thyroid cartilage centroid size of three age groups (pups, young adults, and old adults) and against the first and second shape axis, respectively (PC 1 and PC 2).

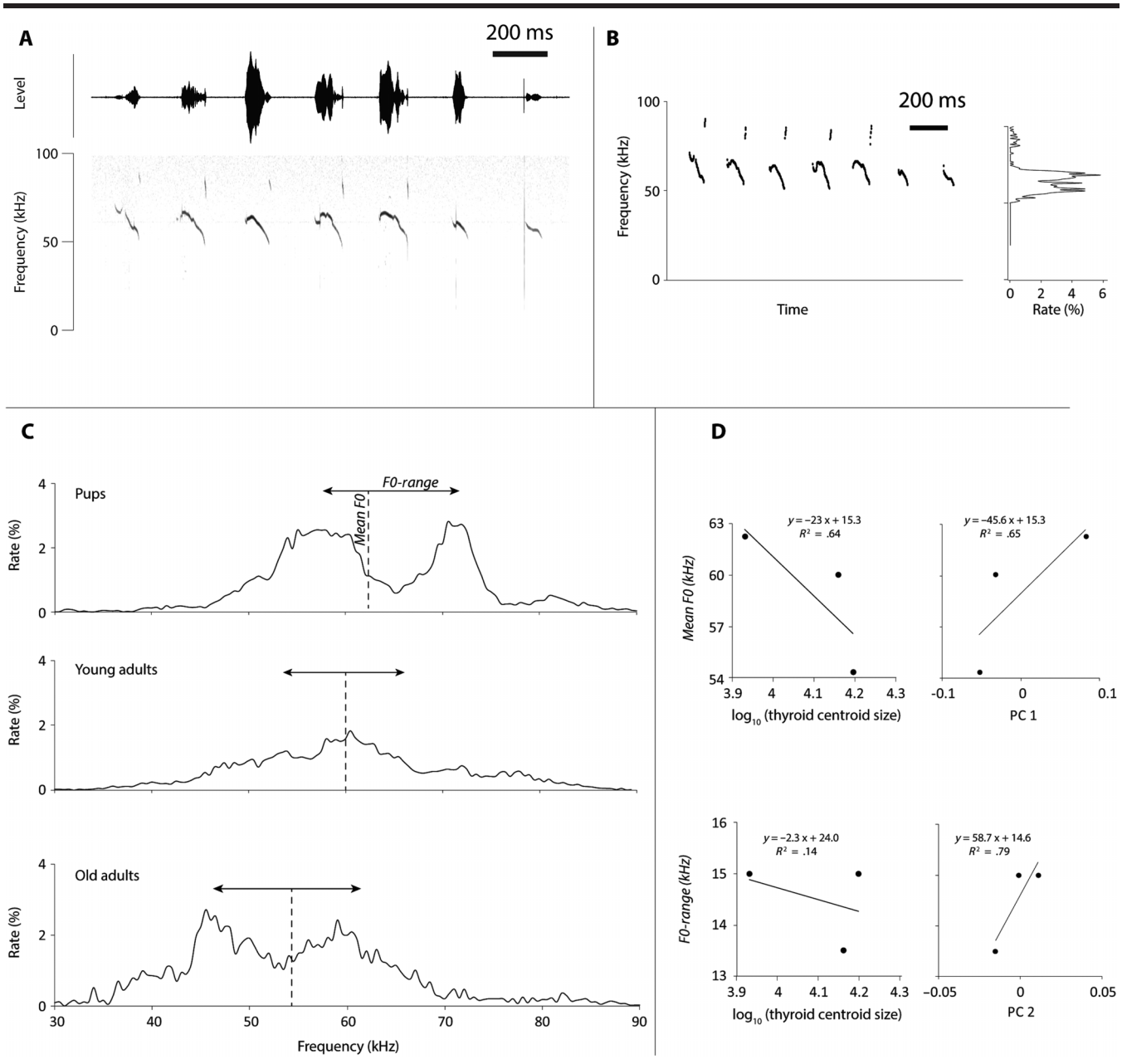

investigators noted that variation for the cricoid cartilage was smaller than for thyroid and arytenoid cartilages (Eckel et al., 1994, 1999; Kahane, 1982). In particular, around puberty, when the male larynx experiences a characteristic increase in overall size, thyroid and arytenoid cartilage experience a greater increase in linear dimensions than the cricoid cartilage (Kahane, 1982).

The greater similarity of cricoid cartilage shape between species was interpreted as reflecting greater functional constraints acting on the cricoid cartilage (Borgard et al., 2019). The cricoid plays a prominent role in laryngeal biomechanics. It forms a complete and robust ring structure and thereby serves to maintain airway patency. It also provides attachment points for three important intrinsic muscles

Downloaded from: https://pubs.asha.org Midwestern University, Illinois on 05/26/2021, Terms of Use: https://pubs.asha.org/pubs/rights_and_permissions

Table 5. Pearson correlation coefficients testing the relationship between two acoustic parameters (mean fundamental frequency [F0], mean F0 and F0 range, F0 range) and various size and shape parameters.

Size parameters	Mean F0	F0-range
Log_{10}(Body mass)	$R = -.83$, $p = .38$	$R = -.34$, $p = .78$
Log_{10}(Femur length)	$R = -.77$, $p = .45$	$R = -.44$, $p = .71$
Log_{10}(Centroid size thyroid)	$R = -.80$, $p = .41$	$R = -.38$, $p = .75$
Log_{10}(Centroid size cricoid)	$R = -.80$, $p = .41$	$R = -.38$, $p = .75$
Log_{10}(Centroid size arytenoid)	$R = -.77$, $p = .44$	$R = -.47$, $p = .72$
Log_{10}(Centroid size epiglottis)	$R = -.83$, $p = .38$	$R = -.34$, $p = .78$
Log_{10}(Ventral pouch latero-lateral distance)	$R = .16$, $p = .88$	$R = .92$, $p = .19$
Log_{10}(Ventral pouch rostro-caudal distance)	$R = -.91$, $p = .18$	$R = -.18$, $p = .81$
Shape parameters		
PC 1 thyroid cartilage	$R = .81$, $p = .40$	$R = .37$, $p = .75$
PC 2 thyroid cartilage	$R = -.66$, $p = .54$	$R = .89$, $p = .30$
PC 1 cricoid cartilage	$R = -.95$, $p = .21$	$R = .54$, $p = .63$
PC 2 cricoid cartilage	$R = .24$, $p = .85$	$R = .88$, $p = .31$
PC 1 arytenoid cartilage	$R = .87$, $p = .33$	$R = .26$, $p = .83$
PC 2 arytenoid cartilage	$R = -.14$, $p = .91$	$R = -.93$, $p = .25$
PC 1 epiglottis	$R = .99$, $p = .11$	$R = -.08$, $p = .95$
PC 2 epiglottis	$R = .07$, $p = .95$	$R = .95$, $p = .20$

as well as ligaments, which function in ab- and adduction of the vocal folds. Each half of the lateral lamina of the cricoid cartilage shows a facet for articulation of the caudal horns of the thyroid cartilage (i.e., the cricothyroid joint). The craniodorsal surfaces contain facets for articulation with the base of the arytenoid cartilages via true joints, which allow rotation of the arytenoid cartilages facilitating ab- and adduction as well as tensing of vocal folds. Those functions could constrain shape variation of the cricoid cartilage within and among species, more than for the other three laryngeal cartilages.

An important feature of the mouse larynx is the presence of a supraglottal but intralaryngeal cavity, known as the ventral pouch (Riede et al., 2017). The ventral pouch branches off from the main airway and plays a critical role in ultrasonic vocal production (Riede et al., 2017). During ultrasonic vocalization, a glottal airflow is guided over the opening of the ventral pouch and impinges on the cartilage re-enforced alar edge situated opposite the glottal exit. This generates a pressure fluctuation between the ventral pouch cavity and the main airway, which, in turn, resonates with the ventral pouch cavity. In an earlier study, we speculated that sound frequency is determined by the airflow speed exiting the glottis, dimensions of the ventral pouch, and the distance between glottal exit and alar edge (Riede et al., 2017). Results of the current investigation support this hypothesis. As expected, ventral pouch size, at least the rostrocaudal dimension, was tightly linked to body size and thyroid cartilage size. This was associated with a size-dependent change of mean F0. A larger ventral pouch supports lower mean F0. Interestingly, the latero-lateral dimension of the ventral pouch did not follow body or thyroid cartilage size, which suggests that parts of the ventral pouch shape are size independent. F0 range was also not clearly related to size but did seem to track variation on PC 2 as well as the latero-lateral dimension of the ventral pouch, perhaps suggesting a form–function relationship between thyroid cartilage, ventral pouch shape, and this acoustic parameter. Ultrasonic vocalizations of mouse models of several neurodevelopmental disorders are used as phenotypic markers (Scattoni et al., 2009). An understanding of how variation in those sounds are generated will determine how this behavior is evaluated.

In summary, it seems that none of the four cartilages escaped the allometric constraints dictated by respiration. However, three of the four cartilages show significant shape changes over ontogeny and the arytenoid and epiglottic cartilages undergo distinct developmental phases in which shape changes disproportionately to growth. In other words, there is some dissociation between growth and development in these cartilages. Integration of those shape changes between cartilages and their functional relevance will be discussed next.

Modular Signals Between Laryngeal Elements Point to Developmental Precursors

The mesoderm-derived cricoid cartilage demonstrated negative allometry but minimal shape difference across developmental stages. This contrasts with the greater phenotypic variation associated with development for the mesoderm-derived arytenoid and epiglottic cartilages as well as the thyroid cartilage, which is of mixed mesoderm and neural crest origin.

The relatively low CR and a large effect size (Z_{CR}) for the pairing of thyroid and cricoid cartilages together suggest their shapes vary with the greatest degree of independence within the larynx. Furthermore, cartilage pairs that featured the thyroid cartilage had the strongest signal of modularity. These observations were interpreted as confirming a greater independence of the thyroid cartilage, which supports the hypothesis that embryological origin influences developmental integration of the larynx. The Z_{CR} value for arytenoid and epiglottic cartilages indicate

Downloaded from: https://pubs.asha.org Midwestern University, Illinois on 05/26/2021, Terms of Use: https://pubs.asha.org/pubs/rights_and_permissions

the weakest modularity signal for this pair. This is likely because of their greater shape integration over development as reflected in their similar u-shaped (nonlinear) developmental trajectories. There are changes that characterize the weanling and young adult stages to the exclusion of the pups and old adults in both cartilages.

An important question deserving further investigation is how functional integrity is maintained in the face of developmental modularity. For example, one might hypothesize that thyroid and arytenoid cartilages would demonstrate strong integration of shape because both structures represent attachment points for the vocal folds. Strong shape integration would then act to maintain functional congruence between these structures to ensure normal function of the laryngeal valve. Yet, the thyroid and arytenoid cartilages demonstrate a modular architecture and distinct patterns of shape development that do not support a hypothesis of strong morphological integration. We suggest that further analyses need to look at subregions of each cartilage to better assess local functional constraints, for example, one of the joint regions (e.g., Storck & Unteregger, 2018).

Conclusions

Laryngeal growth is associated with characteristic changes in shape of four individual cartilages. A test for modular integration suggests that shape changes occur semi-autonomously for all pairs of cartilages, with greater modularity for pairs involving the thyroid cartilage and less for the arytenoid and epiglottic cartilages. The latter two cartilages demonstrate similar nonlinear patterns of shape development that are dissociated to some extent with growth. The study demonstrates how an approach of 3D reconstruction and geometric morphometrics can help tease apart subtle scaling trends, developmental shape trajectories, and patterns of covariation in the larynx.

Our study provides an example of a direct investigation and application of morphometric techniques to understand developmental changes of laryngeal structure and the possible consequences of these changes to functionality. A full understanding of human laryngeal behavior and disorder is deeply rooted in developmental biology. Therefore, our study not only represents a critical step in appreciating human laryngeal behavior in the comparative context of mammalian behavior but also illustrates a novel methodology to address questions of development, growth, and functional consequences (i.e., for teasing out structural factors underlying human voice disorders).

Acknowledgment

This study was funded by the National Science Foundation (IOS 1754332 awarded to T. R.).

References

Adams, D. C. (2016). Evaluating modularity in morphometric data: Challenges with the RV coefficient and a new test measure. *Methods in Ecology and Evolution, 7*(5), 565–572. https://doi.org/10.1111/2041-210X.12511

Adams, D. C., & Collyer, M. L. (2019). Comparing the strength of modular signal, and evaluating alternative modular hypotheses, using covariance ratio effect sizes with morphometric data. *Evolution, 73*(12), 2352–2367. https://doi.org/10.1111/evo.13867

Adams, D. C., Collyer, M. L., Kaliontzopoulou, A., & Sherratt, E. (2017). *Geomorph: Software for geometric morphometric analyses.* R package version 3.0.5. https://cran.r-project.org/package=geomorph

Alli, O., Berzofsky, C., Sharma, S., & Pitman, M. J. (2013). Development of the rat larynx: A histological study. *Laryngoscope, 123*(12), 3093–3098. https://doi.org/10.1002/lary.24145

Baab, K. L., McNulty, K. P., & Rohlf, J. (2012). The shape of human evolution: A geometric morphometrics perspective. *Evolutionary Anthropology, 21*(4), 151–165. https://doi.org/10.1002/evan.21320

Borgard, H., Baab, K. L., Pasch, B., & Riede, T. (2019). The shape of sound: A geometric morphometrics approach to larynx morphology. *Journal of Mammalian Evolution*. Advance online publication. https://doi.org/10.1007/s10914-019-09466-9

Branchi, I., Santucci, D., & Alleva, E. (2001). Ultrasonic vocalisation emitted by infant rodents: A tool for assessment of neurobehavioural development. *Behavioural Brain Research, 125*(1–2), 49–56. https://doi.org/10.1016/S0166-4328(01)00277-7

Brudzynski, S. M. (Ed.) (2018). *Handbook of ultrasonic vocalization: A window into the emotional brain* (Vol. 25). Academic Press.

Campbell, P., Pasch, B., Warren, A. L., & Phelps, S. M. (2014). Vocal ontogeny in neotropical singing mice (*Scotinomys*). *PLOS ONE, 9*(12), e113628. https://doi.org/10.1371/journal.pone.0113628

Dalal, P. G., Murray, D., Messner, A. H., Feng, A., McAllister, J., & Molter, D. (2009). Pediatric laryngeal dimensions: An age-based analysis. *Anesthesia & Analgesia, 108*(5), 1475–1479. https://doi.org/10.1213/ane.0b013e31819d1d99

Dent, M. L., Fay, R. R., & Popper, A. N. (2018). *Rodent bioacoustics*. Springer. https://link.springer.com/book/10.1007/978-3-319-92495-3

Dutschmann, M., Mörschel, M., Rybak, I. A., & Dick, T. E. (2009). Learning to breathe: Control of the inspiratory–expiratory phase transition shifts from sensory- to central-dominated during postnatal development in rats. *Journal of Physiology, 587*(20), 4931–4948. https://doi.org/10.1113/jphysiol.2009.174599

Eckel, H. E., Sittel, C., Zorowka, P., & Jerke, A. (1994). Dimensions of the laryngeal framework in adults. *Surgical and Radiologic Anatomy, 16,* 31–36. https://doi.org/10.1007/BF01627918

Eckel, H. E., Sprinzl, G. M., Koebke, J., Pototschnig, C., Sittel, C., & Stennert, E. (1999). Morphology of the human larynx during the first five years of life studied on whole organ serial sections. *Annals of Otology, Rhinology & Laryngology, 108*(3), 232–237. https://doi.org/10.1177/000348949910800303

Eckenhoff, J. E. (1951). Some anatomic considerations of the infant larynx influencing endotracheal anesthesia. *Anesthesiology: The Journal of the American Society of Anesthesiologists, 12*(4), 401–410.

Fernández-Vargas, M. (2018). Vocal signals of sexual motivation in male and female rodents. *Current Sexual Health Reports, 10*(4), 315–328. https://doi.org/10.1097/00000542-195107000-00001

Flurkey, K., Currer, J. M., & Harrison, D. E. (2017). Mouse models in aging research. In J. G. Fox, S. W. Barthold, M. T. Davisson, C. E. Newcomer, F. W. Quimby, & A. L. Smith (Eds.), *The mouse in biomedical research*. Elsevier.

Fröhlich, H., Rafiullah, R., Schmitt, N., Abele, S., & Rappold, G. A. (2017). Foxp1 expression is essential for sex-specific murine

Downloaded from: https://pubs.asha.org Midwestern University, Illinois on 05/26/2021, Terms of Use: https://pubs.asha.org/pubs/rights_and_permissions

neonatal ultrasonic vocalization. *Human Molecular Genetics, 26*(8), 1511–1521. https://doi.org/10.1093/hmg/ddx055

Gower, J. C. (1975). Generalized Procrustes analysis. *Psychometrika, 40,* 33–51. https://doi.org/10.1007/BF02291478

Hallgrímsson, B., Lieberman, D. E., Liu, W., Ford-Hutchinson, A. F., & Jirik, F. R. (2007). Epigenetic interactions and the structure of phenotypic variation in the cranium. *Evolution & Development, 1,* 76–91. https://doi.org/10.1111/j.1525-142X.2006.00139.x

Haney, M. M., Hamad, A., Woldu, H. G., Ciucci, M., Nichols, N., Bunyak, F., & Lever, T. E. (2020). Recurrent laryngeal nerve transection in mice results in translational upper airway dysfunction. *Journal of Comparative Neurology, 528*(4), 574–596. https://doi.org/10.1002/cne.24774

Heude, E., Tesarova, M., Sefton, E. M., Jullian, E., Adachi, N., Grimaldi, A., Zikmund, T., Kaiser, J., Kardon, G., Kelly, R. G., & Tajbakhsh, S. (2018). Unique morphogenetic signatures define mammalian neck muscles and associated connective tissues. *eLife, 7,* e40179.

Hoh, J. F. Y. (2005). Laryngeal muscle fibre types. *Acta Physiol Scandinavica, 183*(2), 133–149. https://doi.org/10.7554/eLife.40179

Holy, T. E., & Guo, Z. (2005). Ultrasonic songs of male mice. *PLOS BIOLOGY, 3*(12), e386. https://doi.org/10.1371/journal.pbio.0030386

Holzki, J., Brown, K. A., Carroll, R. G., & Cote, C. J. (2018). The anatomy of the pediatric airway: Has our knowledge changed in 120 years? A review of historic and recent investigations of the anatomy of the pediatric larynx. *Pediatric Anesthesia, 28*(1), 13–22. https://doi.org/10.1111/pan.13281

Kahane, J. C. (1982). Growth of the human prepubertal and pubertal larynx. *Journal of Speech and Hearing Research, 25*(3), 446–455. https://doi.org/10.1044/jshr.2503.446

Klingenberg, C. P. (2016). Size, shape, and form: Concepts of allometry in geometric morphometrics. *Development Genes and Evolution, 226,* 113–137. https://doi.org/10.1007/s00427-016-0539-2

Litman, R. S., Weissend, E. E., Shibata, D., & Westesson, P.-L. (2003). Developmental changes of laryngeal dimensions in unparalyzed, sedated children. *Anesthesiology, 98*(1), 41–45. https://doi.org/10.1097/00000542-200301000-00010

Lungova, V., Verheyden, J. M., Herriges, J., Sun, X., & Thibeault, S. L. (2015). Ontogeny of the mouse vocal fold epithelium. *Developmental Biology, 399*(2), 263–282. https://doi.org/10.1016/j.ydbio.2014.12.037

McMullen, C. A., Butterfield, T. A., Dietrich, M., Andreatta, R. D., Andrade, F. H., Fry, L., & Stemple, J. C. (2011). Chronic stimulation-induced changes in the rodent thyroarytenoid muscle. *Journal of Speech, Language, and Hearing Research, 54*(3), 845–853. https://doi.org/10.1044/1092-4388(2010/10-0127)

Montalbano, M. B., Hernández-Morato, I., Tian, L., Yu, V. X., Dodhia, S., Martinez, J., & Pitman, M. J. (2019). Recurrent laryngeal nerve reinnervation in rats posttransection: Neurotrophic factor expression over time. *Otolaryngology—Head and Neck Surgery, 161*(1), 111–117. https://doi.org/10.1177/0194599819831289

Mortola, J. P., & Fisher, J. T. (1980). Comparative morphology of the trachea in newborn mammals. *Respiration Physiology, 39*(3), 297–302. https://doi.org/10.1016/0034-5687(80)90061-4

Neubauer, S., Gunz, P., & Hublin, J.-J. (2010). Endocranial shape changes during growth in chimpanzees and humans: A morphometric analysis of unique and shared aspects. *Journal of Human Evolution, 59*(5), 555–566. https://doi.org/10.1016/j.jhevol.2010.06.011

O'Leary, M. A., & Kaufman, S. G. (2012). *MorphoBank 3.0: Web application for morphological phylogenetics and taxonomy*. http://www.morphobank.org

Olson, E. C., & Miller, R. L. (1958). *Morphological integration*. University of Chicago.

Peterson, J. R., Watts, C. R., Morris, J. A., Shelton, J. M., & Cooper, B. G. (2013). Laryngeal aging and acoustic changes in male rat ultrasonic vocalizations. *Developmental Psychobiology, 55*(8), 818–828. https://doi.org/10.1002/dev.21072

R Core Team. (2015). *R: A language and environment for statistical computing. R Foundation for Statistical Computing, Vienna, Austria*. https://www.R-project.org/

Riede, T. (2011). Subglottal pressure, tracheal airflow, and intrinsic laryngeal muscle activity during rat ultrasound vocalization. *Journal of Neurophysiology, 106*(5), 2580–2592. https://doi.org/10.1152/jn.00478.2011

Riede, T. (2013). Call type specific motor patterns in rat ultrasound vocalization. *Journal of Experimental Zoology A, 319,* 213–224.

Riede, T. (2018). Peripheral vocal motor dynamics and combinatory call complexity of ultrasonic vocal production in rats. In S. M. Brudzynski (Ed.), *Handbook of ultrasonic vocalization* (Vol. 25, pp. 45–60). Elsevier. https://doi.org/10.1016/B978-0-12-809600-0.00005-6

Riede, T., Borgard, H., & Pasch, B. (2017). Laryngeal airway reconstruction indicates rodent ultrasonic vocalizations are produced by an edge-tone mechanism. *Royal Society Open Science, 4*(11), 170976. https://doi.org/10.1098/rsos.170976

Rohlf, F. J., & Slice, D. (1990). Extension of the Procrustes method for the optimal superimposition of landmarks. *Systematic Zoology, 39*(1), 40–59. https://doi.org/10.2307/2992207

Russell, J. A., Ciucci, M. R., Hammer, M. J., & Connor, N. P. (2013). Videofluorographic assessment of deglutitive behaviors in a rat model of aging and Parkinson disease. *Dysphagia, 28*(1), 95–104. https://doi.org/10.1007/s00455-012-9417-x

Sang, Q., & Goyal, R. K. (2001). Swallowing reflex and brain stem neurons activated by superior laryngeal nerve stimulation in the mouse. *American Journal of Physiology—Gastrointestinal and Liver Physiology, 280*(2), G191–G200. https://doi.org/10.1152/ajpgi.2001.280.2.G191

Scattoni, M. L., Crawley, J., & Ricceri, L. (2009). Ultrasonic vocalization: A tool for behavioural phenotyping of mouse models of neurodevelopmental disorders. *Neuroscience & Biobehavioral Reviews, 33*(4), 508–515. https://doi.org/10.1016/j.neubiorev.2008.08.003

Sittel, C. (2014). Pathologies of the larynx and trachea in childhood. *GMS Current Topics in Otorhinolaryngology, Head and Neck Surgery, 13,* 09.

Storck, C., & Unteregger, F. (2018). Cricothyroid joint type as predictor for vocal fold elongation in professional singers. *Laryngoscope, 128*(5), 1176–1181. https://doi.org/10.1002/lary.26984

Tabler, J. M., Rigney, M. M., Berman, G. J., Gopalakrishnan, S., Heude, E., Al-Lami, H. A., Yannakoudakis, B. Z., Fitch, R. D., Carter, C., Vokes, S., Liu, K. J., Tajbakhsh, S., Egnor, S. E. R., & Wallingford, J. B. (2017). Cilia-mediated Hedgehog signaling controls form and function in the mammalian larynx. *elife, 6,* e19153. https://doi.org/10.7554/eLife.19153

Tateya, T., Tateya, I., Sohn, J. H., & Bless, D. M. (2005). Histologic characterization of rat vocal fold scarring. *Annals of Otology, Rhinology & Laryngology, 114*(3), 183–191. https://doi.org/10.1177/000348940511400303

Tayama, N., Kaga, N., Chan, R. W., & Titze, I. R. (2001). Geometric characterization of the laryngeal cartilage framework for the purpose of biomechanical modeling. *Annals of Otology, Rhinology & Laryngology, 110*(12), 1154–1161. https://doi.org/10.1177/000348940111001213

Downloaded from: https://pubs.asha.org Midwestern University, Illinois on 05/26/2021, Terms of Use: https://pubs.asha.org/pubs/rights_and_permissions

Tenney, S. M., & Bartlett, D., Jr. (1967). Comparative quantitative morphology of the mammalian lung: Trachea. *Respiration Physiology, 3*(2), 130–135. https://doi.org/10.1016/0034-5687(67)90002-3

Thomas, L. B., Stemple, J. C., Andretta, R. D., & Andrade, F. H. (2009). Establishing a new animal model for the study of laryngeal biology and disease: An anatomic study of the mouse larynx. *Journal of Speech, Language, and Hearing Research, 52*(3), 802–811. https://doi.org/10.1044/1092-4388(2008/08-0087)

Titze, I. R. (2000). *Principals of voice production*. National Center for Voice and Speech.

Tobias, J. D. (2015). Pediatric airway anatomy may not be what we thought: Implications for clinical practice and the use of cuffed endotracheal tubes. *Pediatric Anesthesia, 25*(1), 9–19. https://doi.org/10.1111/pan.12528

Turman, J. E. (2007). The development of mastication in rodents: From neurons to behaviors. *Archives of Oral Biology, 52*(4), 313–316. https://doi.org/10.1016/j.archoralbio.2006.08.013

Valerius, K.-P. (1996). Size-dependent morphology of the conductive bronchial tree in four species of myomorph rodents. *Journal of Morphology, 230*(3), 291–297. https://doi.org/10.1002/(SICI)1097-4687(199612)230:3<291::AID-JMOR4>3.0.CO;2-H

Wagner, G. P. (1996). Homologues, natural kinds and the evolution of modularity. *American Zoologist, 36*(1), 36–43. https://doi.org/10.1093/icb/36.1.36

Watts, C. R., Marler, J. A., & Rousseau, B. (2011). Qualitative characterization of elastic fiber distribution in the mouse vocal fold: Further development of an animal model. *Journal of Voice, 25*(1), e1–e6. https://doi.org/10.1016/j.jvoice.2009.07.010

Welham, N. V., Ling, C., Dawson, J. A., Kendziorski, C., Thibeault, S. L., & Yamashita, M. (2015). Microarray-based characterization of differential gene expression during vocal fold wound healing in rats. *Disease Models and Mechanisms, 8,* 311–321. https://doi.org/10.1242/dmm.018366

Yamashita, M., Bless, D. M., & Welham, N. V. (2010). Morphological and extracellular matrix changes following vocal fold injury in mice. *Cells Tissues Organs, 192,* 262–271. https://doi.org/10.1159/000315476

Zala, S. M., Reitschmidt, D., Noll, A., Balazs, P., & Penn, D. J. (2017). Sex-dependent modulation of ultrasonic vocalizations in house mice (*Mus musculus musculus*). *PLOS ONE, 12*(12), e0188647. https://doi.org/10.1371/journal.pone.0188647

Zelditch, M. L., Lundrigan, B. L., & Garland, T., Jr. (2004). Developmental regulation of skull morphology. I. Ontogenetic dynamics of variance. *Evolution and Development, 6*(3), 194–206. https://doi.org/10.1111/j.1525-142X.2004.04025.x

Downloaded from: https://pubs.asha.org Midwestern University, Illinois on 05/26/2021, Terms of Use: https://pubs.asha.org/pubs/rights_and_permissions